Cosmic ray driven dynamo in barred galaxies - 3D numerical simulations

N. Nowak[1], K. Kulba-Dybeł[1], K. Otmianowska-Mazur[1], M. Hanasz[2], H. Siejkowski[1], B. Kulesza-Żydzik[1].

(1) Astronomical Observatory of the Jagiellonian University, ul. Orla 171, 30-244 Kraków, Poland

(2) Centre for Astronomy, Nicolaus Copernicus University, Faculty Physics, Astronomy and Informatics, Grudziadzka 5, PL 87100 Toruń, Poland

Abstract

Our MHD numerical calculations provide results for a three-dimensional model of barred galaxies involving a cosmic-ray driven dynamo process that depends on star formation rates. Furthermore, we argue that the cosmic-ray driven dynamo can account for a number of magnetic features in barred galaxies, such as magnetic arms observed along the gaseous arms, magnetic arms in the inter-arm regions, polarized emission that is at the strongest in the central part of the galaxy, where the bar is situated, polarized emission that forms ridges coinciding with the dust lanes along the leading edges of the bar, as well as their very strong total radio intensity. Our results give the modelled magnetic field topology similar to the observational maps of polarized intensity in barred galaxies. Moreover, they cast a new light on a number of polarization properties observed in barred or even spiral galaxies, like fast exponential growth of the total magnetic energy to the present values, stochastic nature of magnetic field reversals (for instance: in the Milky Way). We concluded that a cosmic-ray driven dynamo process in barred galaxies could boost magnetic fields efficiently. The fastest rate of magnetic field increase is 195 yr for SN frequency 1/50 yr⁻¹. The obtained intensity of magnetic field corresponds to the observational values (few μG in spiral arms).

Introduction

Radio observations indicate that magnetic fields are important agents in the interstellar medium within both spiral and barred galaxies (Beck 2012). The large-scale structure of magnetic field in such galaxies is generally represented by a superposition of modes with different azimuthal and vertical field directions and symmetries. In the galactic disks, the axisymmetric spiral (ASS) mode is the strongest one (Ruzmaikin et al. 1988), however the bi-symmetric spiral mode (BSS) or a mixture of both with a preponderance of either pattern is also observed (Beck et al. 1996). The vertical symmetry can be even (quadrupole) or odd (bipolar). Rotation measure observations show that the ASS magnetic field is present in several galaxies, e.g., in M31 (Sofue & Takano 1981) or IC 342 (Sokoloff et al. 1992).

The BSS mode was unequivocally observed just in one galaxy, M81 (Sokoloff et al. 1992). Many other observations indicate that the BSS mode can occur along ASS mode, e.g. in M33 or NGC 4631 (Hummel et al. 1991). According to the magnetohydrodynamical (MHD) dynamo theory, the galactic magnetic fields should have the even symmetry rather than the odd one, and the global magnetic fields of spherical objects (including stars and planets) are mostly dipolar, while those of flattened objects (spiral galaxies) are quadrupolar (Krause 2004).

Although a distinct ASS or BSS mode was detected in several galaxies, most of magnetic field structures seem to be a superposition of the different dynamo modes (Beck 2012). This could be due to many processes occurring in disks of galaxies, which may be correlated with the MHD dynamo process.

Model

The computations of evolution of a barred galaxy are done by solving the isothermal non-ideal MHD equations of the form

$$\frac{\partial \rho}{\partial t} + \nabla \cdot (\rho \vec{v}) = 0, \tag{1}$$

$$\frac{\partial \vec{v}}{\partial t} + (\vec{v} \cdot \nabla)\vec{v} = -\frac{1}{\rho}\nabla\left(p + p_{cr} + \frac{B^2}{8\pi}\right) + \frac{\vec{B} \cdot \nabla \vec{B}}{4\pi\rho} - \nabla\Phi, \tag{2}$$

$$\frac{\partial \vec{B}}{\partial t} = \nabla \times (\vec{v} \times \vec{B} - \eta\nabla \times \vec{B}), \tag{3}$$

$$\nabla \cdot \vec{B} = 0, \tag{4}$$

where $\vec{v}$ is the large-scale velocity of gas, ρ is the gas density distribution, p is the gas pressure, p_{cr} is the cosmic-ray pressure, Φ is the gravitational potential, $\vec{B}$ is the magnetic induction, e is the thermal energy density and η is the turbulent magnetic diffusivity. An isothermal equation of state was assumed, that is $p = \rho c_s^2$, where c_s is the isothermal speed of sound.

We investigated the problem of propagation of CR transport ((Schlickeiser & Lerche 1985)) in the ISM by solving the following diffusion-advection equation:

$$\frac{\partial e_{cr}}{\partial t} + \nabla \cdot (e_{cr}\vec{v}) = \nabla(\hat{K}\nabla e_{cr}) - p_{cr}(\nabla \cdot \vec{v}) + CR_{source}, \tag{5}$$

where e_{cr} is the cosmic ray energy density, $p_{cr} = (\gamma_{cr} - 1)e_{cr}$ is the cosmic ray pressure, $\hat{K}$ is the diffusion tensor, $\vec{v}$ is the gas velocity and CR_{source} is the source term for the cosmic-ray energy. Moreover, we assume that 10% of 10^{51} erg of the SNe kinetic energy from their outburst is transformed into the CR energy and leave out the thermal energy, applying the value of adiabatic index for the CR gas as $\gamma_{cr} = 14/9$ and adding the CRs pressure to the total pressure in the ISM gas motion equation as ∇p_{cr} (Berezinski et al. 1990). It is also assumed that the CR gas diffuses anisotropically (Ryu et al. 2003). The CR diffusion tensor K is defined as:

$$K_{ij} = K_\perp \delta_{ij} + (K_\parallel - K_\perp)n_i n_j, \tag{6}$$

where $K_\perp$ and $K_\parallel$ are the parallel and perpendicular (with respect to the local magnetic field direction) cosmic-ray diffusion coefficients and $n_i = B_i/B$ are components of unit vectors tangent to the magnetic field lines.

TABLE 1: Parameters adopted for the barred galaxy model.

parameter	meaning	value	units
M_d	disk mass	$4.0 \cdot 10^{10}$	$M_\odot$
a_d	length scale of the disk	0.6	kpc
M_b	bulge mass	$1.5 \cdot 10^{10}$	$M_\odot$
a_b	length scale of the bulge	5.0	kpc
M_h	halo mass	$1.2 \cdot 10^{11}$	$M_\odot$
a_h	length scale of the halo	15.0	kpc
M_{bar}	bar mass	$1.5 \cdot 10^{10}$	$M_\odot$
a_{bar}	length scale of bar major axis	6.0	kpc
b_{bar}	length scale of bar minor axis	3.0	kpc
c_{bar}	length scale of bar vertical axis	2.5	kpc
Ω_{bar}	bar angular velocity	30.0	km s⁻¹kpc⁻¹
CR	corotation radius	6.0	kpc
IILR	Inner Inner Lindblad Resonance	0.4	kpc
OILR	Outer Inner Lindblad Resonance	3.0	kpc
OLR	Outer Lindblad Resonance	8.5	kpc
R_{BG}	galaxy radius	13.5	kpc

Results

In four experiments, S25, S50, S200 and S500, the magnetic field in vicinity of the disk and and the halo of the barred galaxy was of even (quadrupole-like) symmetry. An odd (dipole-type) configuration of magnetic field with respect to the galactic plane appeared in all the models at an early stage of evolution. This picture is supported by theoretical studies (e.g. Ruzmaikin et al. 1988), by observational evidence (e.g. Heesen et al. 2009), as well as by a number of numerical investigations (e.g. Brandenburg et al. 1993).

However, only in the S100 model ($f_{SN} = 1/100 \, \text{yr}^{-1}$), such a configuration was observed during the entire simulation time. The variable polarity of magnetic field apparent in the horizontal slice showing model S100 is caused by the corrugated surface dividing the regions of positive and negative azimuthal magnetic fields. The odd symmetry of magnetic field is not the preferred configuration in the disk geometry ((Moss et al. 2010)), while it has been found in some galaxies (e.g. in NGC 4631, (Krause 2003)).

MODEL S200   MODEL S100
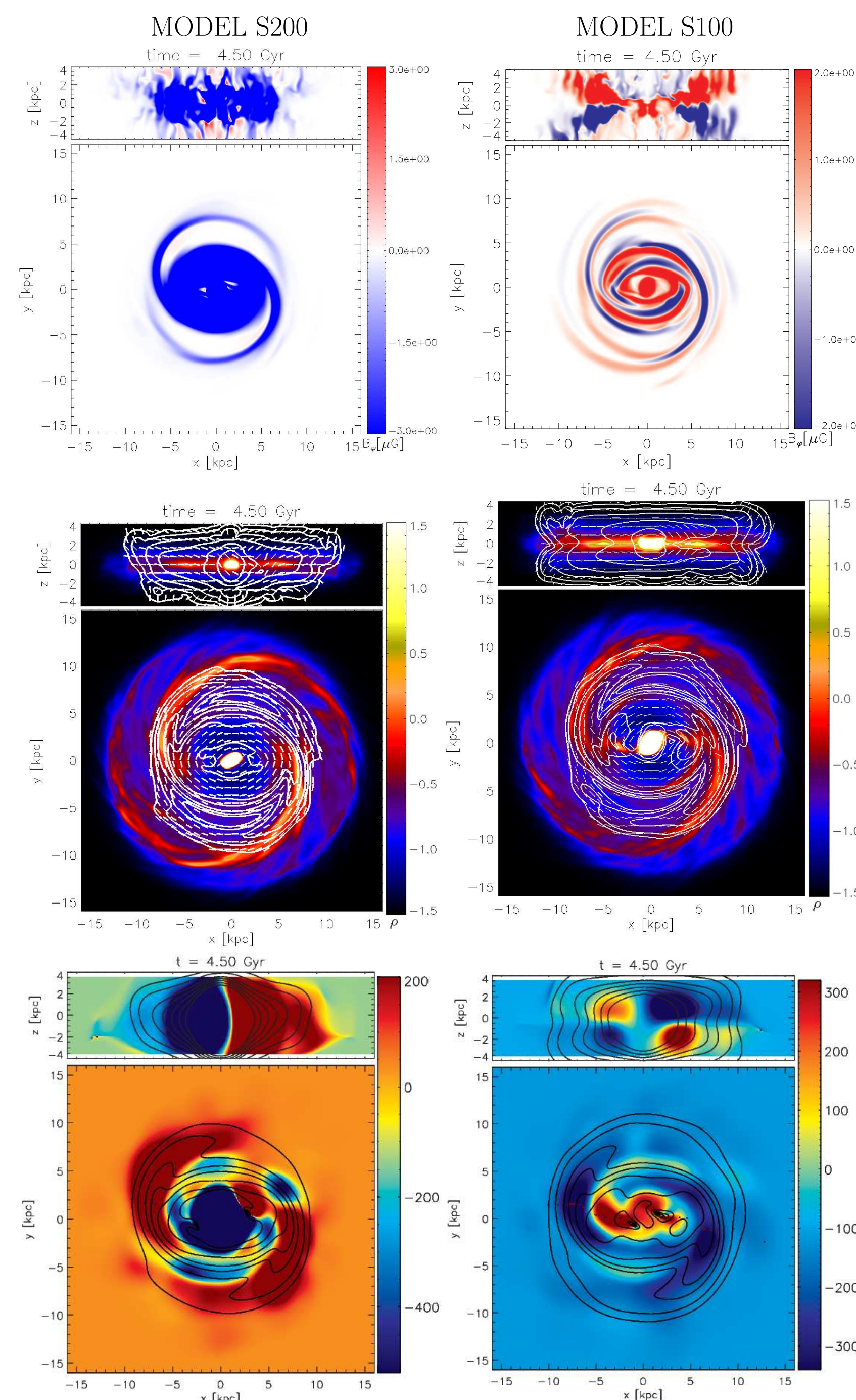
FIG. 2: Top panels: Distribution of toroidal magnetic field in vertical and horizontal slices through the disk centre for models: S200 (left panel) and S100 (right panel). Red colour represents regions with positive toroidal magnetic field, blue with negative, while unmagnetized regions are white. In order to enhance weaker magnetic field structures in the outer galactic disk (e.g. magnetic arms), the colour scale in the magnetic field maps is saturated. Middle panels: Face-on and edge-on polarization maps for the selected time steps. Polarized intensity (contours) and polarization angles (dashes) are superimposed onto the column density plots. Bottom panels: Faraday rotation maps for selected times steps. The red area denotes the positive RM and blue area denotes the negative RM.

Magnetic arms between the gaseous spiral and the bar have been observed in most of the barred galaxy simulations. The drift of magnetic arms could be explained as follows: initially the gravitational potential of the bar rotates faster than the gas outside the corotation radius, generating spiral arms. The magnetic field present in the galactic disk is advected with the gas velocity. In particular the magnetic field produced by disturbances within the arms drifts with the gas velocity, and after some time runs into the next arm.
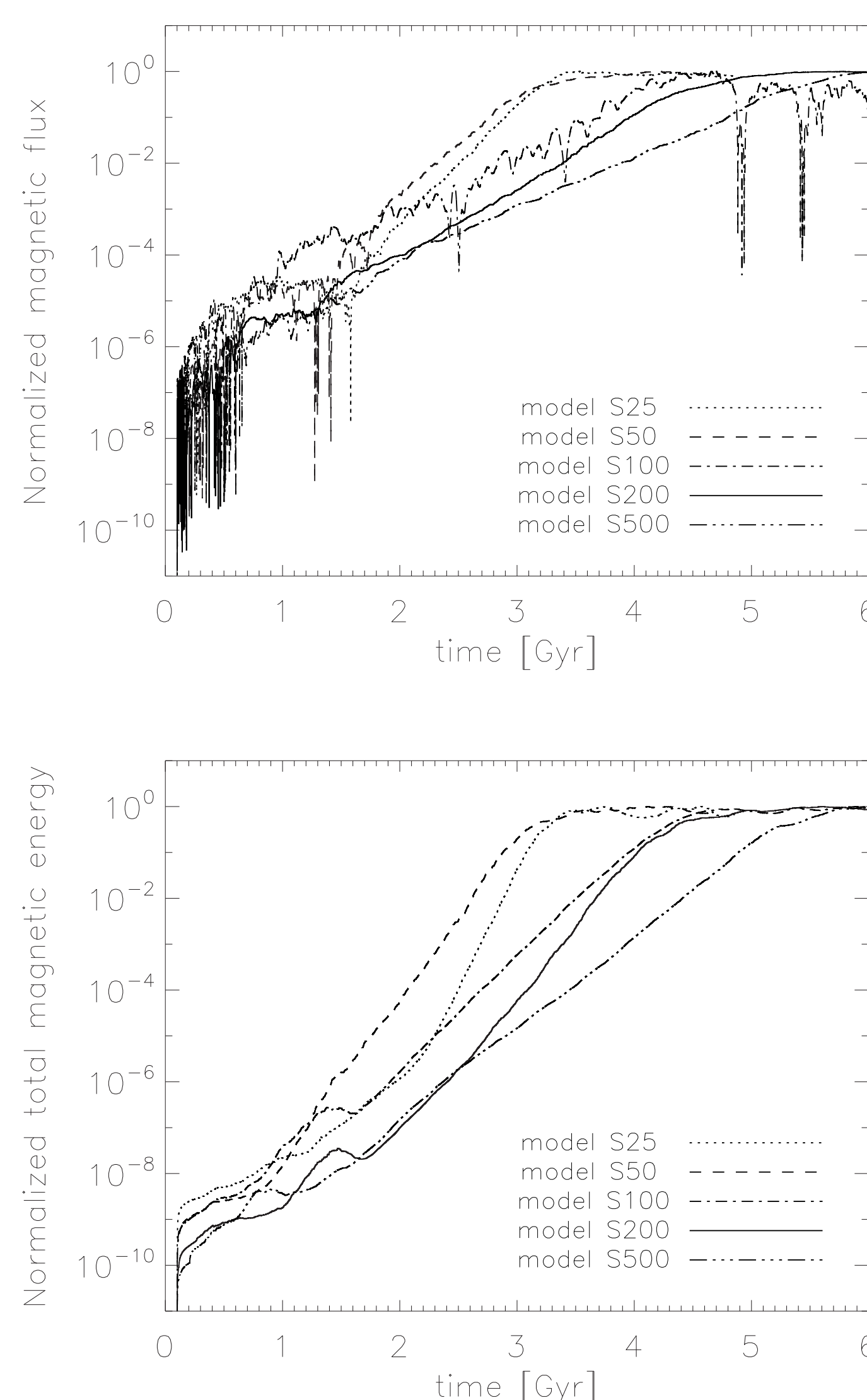
FIG. 3: Evolution of total magnetic energy E_B (top panel) and of mean azimuthal flux B_ϕ (bottom panel) for different values of SN frequency f_{SN}. Both quantities are normalized with respect to the equipartition value.

The mass outflow rate by galactic winds in the barred galaxy simulations ranged from 0.6 to 4.7 $M_\odot \, \text{yr}^{-1}$. The overall rate of mass outflow grew with increasing SN activity in the galactic disk. The galactic-scale outflows (galactic winds) from galactic disks are common phenomena and can be observed both in the nearby galaxies Tüllmann et al. (2006) and in the high-redshift universe Tapken et al. (2007).

TABLE 4: Overview of the obtained parameters for the barred galaxy models. The columns show respectively: the model name, the SN frequency f_{SN}, e-folding time τ, the rate of the mass outflow M_{lost}, the maximum magnetic field in the galactic arms max B_φ^{arms} and the mean od the total magnetic field (regula and turbulent) B_{mean} (saturation state).

Model	f_{SN} [yr⁻¹]	τ [Myr]	M_{lost} [$M_\odot$ yr⁻¹]	max B_φ^{arms} [μG]	B_{mean} [μG]
S25	1/25	230	4.7	$4.7 \cdot 10^{-2}$	3.7
S50	1/50	194	3.2	2.1	6.4
S100	1/100	326	1.7	5.9	7.1
S200	1/200	300	1.1	9.5	10.2
S500	1/500	360	0.6	8.6	7.9

Conclusions

1. The polarized radio emission found in the face-on synthetic polarization maps indicates that the cosmic-ray driven dynamo can be responsible for various magnetic structures discerned in actual observations of barred galaxies such as: the polarized emission which is at the strongest in the central part of the galaxy, where the bar is present, and the polarized emission from the ridges marking the dust lanes along the leading edges of the bar.

2. In the case of simulated barred galaxies, a drift of magnetic arms can be observed during the entire simulation time in most of the experiments.

3. The synthetic edge-on radio maps of polarized emission show that the cosmic-ray driven dynamo can reproduce the vertical magnetic field structures observed in edge-on galaxies (so-called X-type).

4. In barred galaxies, the large-scale magnetic field grows exponentially in a timescale comparable to that obtained for normal spirals. The fastest amplification of magnetic fields was obtained for the S50 model with a SN frequency of 1/50 yr⁻¹ and with the corresponding e-folding time of 194 Myr.

5. In the case of simulated barred galaxies, there is no significant dependence on the SN rate. We found that after about 1 Gyr from the beginning of evolution of the modelled galaxies, the total magnetic energy did not depend on how much of magnetic field energy from the supernovae remnants we had introduced.

6. According to the theoretical studies, the quadrupole-like symmetry of magnetic field is preferred in numerical studies of the galactic dynamo. The even symmetry of magnetic field with respect to the mid-plane was found in most of barred galaxy simulations. Just one model involved the odd symmetry of magnetic field.

References

Beck, R.,2012, Space Science Rev. V. 166, 215

Beck, R., Brandenburg, A., Moss, D., Shukurov, A. & Sokoloff, D. D., 1996, Annu. Rev. Astron. Astrophys., 34, 155

Berezinski, V. S., Bulanov, S. V., Dogiel, V. A., Ginzburg, V. L., Ptuskin, V. S., Astrophysics of cosmic rays, Amsterdam:North-Holland, 1990.

Brandenburg, A., Donner, K. J., Moss, D. et al., 1993, A&A, 271, 36

Heesen, V., Krause, M., Beck, R. & Dettmar, R. 2009, A&A, 506, 1123

Hummel, E., Beck, R., Dahlem, M. 1991, A&A 248, 23

Krause, M., 2004, In The Magnetized Interstellar Medium, B. Uyaniker, W. Reich, R. Wielebinski (eds.), Conf. Proceed., Antalya

Krause, M., 2003, in Radio Studies of Galactic Objects, Galaxies and AGNs, J.L. Han, X.H. Sun, J. Yang & R. Wielebinski (eds.), Acta Astronomica Sinica, 44

Moss D., Sokoloff, D., Beck, R. & Krause, M., 2010, A&A, 512, 61

Ruzmaikin, A. A., Shukurov, A. M. & Sokoloff, D. D., 1988, Magnetic Fields of Galaxies, Kluwer, Dordrecht

Ryu, D., Kim, J., Hong, S. S. & Jones, T. W., 2003, ApJ, 589, 338

Schlickeiser, R. & Lerche, I., 1985, A&A, 151, 151

Sofue, Y. & Takano, T., 1981., Publ. Astron. Soc. Jpn., 33, 47

Sokoloff, D., Shukurov, A. & Krause M., 1992, A&A, 264, 396

Tapken, C., Appenzeller, I., Noll, S., Richling, S., Heidt, J., Meinköhn, E. & Mehlert, D., 2007, A&A, 467, 63

Tüllmann, R., Pietsch,W., Rossa, J., Breitschwerdt, D. & Dettmar, R.-J. 2006, A&A, 448, 43